SPEED OBSERVER AND MOTION CONTROLLER DESIGN FOR PERMANENT MAGNET SYNCHRONOUS MOTORS

[1]ONUR GÜRLEYEN, [2]ILKER ÜSTOĞLU

[1,2]Department of Control and Automation Engineering, Yıldız Technical University
E-mail: [1]gurleyenonur@gmail.com, [2]ustoglu@yildiz.edu.tr

Abstract - Permanent magnet synchronous motor's (PMSM) three phase stator currents are decomposed into flux generating current and torque generating current using mathematical Park and Clarke transformations and decoupling methods, so that PMSM is controlled like DC motor with high efficiency and with high performance. PMSM is controlled cascaded control structure consisting of three main control loops which are current, speed and position control loops and current loop consists of two loops which are d current, related with flux, and q current, related with torque. One of the most important criteria while designing cascaded control loops is bandwidth. Control loop with higher bandwidth means, lower settling time that defines how fast control is occur. While designing control loops with desired bandwidth, small overshoot is acceptable for current loop; However, overshoot and steady state error for position control loop and for speed control loop are undesirable. Moreover, for low speed application speed observer is necessary, since incremental encoder resolution is decreased in low speed control. According to mentioned problems and design criteria, in that paper it is described that current loop with state feedback decoupling, PID controller with pseudo feedback derivative current controller design, speed control loop with approximate first order transfer function using PI controller with no overshoot and no steady state error, proportional (P) position controller guaranteeing no overshoot in desired bandwidth and that PID liked full order speed observer with approximated first order transfer function.Controllers and observer designs are simulated in Matlab Simulink

Index Terms - PMSM, Motion Control, Cascaded Control, Pseudo Derivative Feedback, State Feedback Decoupling, Bandwidth, Speed observer, Speed Control with no overshoot.

I. INTRODUCTION

Permanent magnet synchronous motor (PMSM) and PMSM driver are widely used in industrial servo systems, automotive powertrain systems, since PMSM's stator current is decomposed into flux generating d current and torque generating q current using mathematical transformation methods so thatPMSM is controlled likeDC motor with higher efficiency and higher performance than DC motor. d and q currents obtained by three phases stator currents are coupled and non-linear, therefore d and q currents are decoupled using state feedback linearization to be controlled by linear controller [2]. Control structure in PMSM servo drives is cascaded control structure consisting of two inner d and q currents loops, mid a speed loops and outer a position loop [1]. In that structure, speed reference is produced by position controller, and current reference is obtained by multiplying coefficient with torque reference, generated by speed controller, and output signal of d and q current controllers represent d and q voltages. By inverse mathematical transformation three phases voltages are obtained by q and d voltages. Generally, PI (Proportional + Integrator) controller for current, for speed and P (Proportional) controllers for position are preferred to maintain desired performance criteria, such as increased bandwidth, no steady state error for step input and no overshoot. Increased bandwidth is essential for servo drives, for that reason while bandwidth of control loop is increased, settling time is decreased and control loops could response to input signal fast. Nowadays, improved servo drives with FPGA achieve less than 1ms settling time for position loop. Moreover, overshoot for position, for speed control, and steady state error to step input for all loops are not desirable and for ramp input to minimize following error feed forward control methods is used. Besides, speed control at low speeds is general problem, since incremental encoder with low resolution generating fewer pulses and number of pulses is decreased generated at unity time. Thus, general speed calculation methods at low speed, such as T method, calculating speed by pulses number in unity time are not effectively work at low speed [3] There are two main methods to increase performance at low speed, that are using absolute encoder, which is expensive solution, and that are using full order Luenberger observer estimating speed and load torque [3]. That Luenberger observer is designed liked position control loops with PID controller with reference signal is actual real position (radian) measured by encoder and with output signal estimated speed (radian/second), and estimated position (radian) which is feedback signal of speed observer, are integrated by estimated speed in radian/seconds. Thus, PID liked full order Luenberger observer gains is set liked designing PID controller for position control with higher bandwidth.

II. MODEL OF PMSM AND DESIGN OF CONTROLLER FOR DESIRED PERFORMANCE CRITERIA

A. Mathematical Model of PMSM

Model of PMSM is obtained with assumption listed below [4]

- Saturations are neglected
- Induced EMF is sinusoidal

- Eddy currents and hysteresis loss are negligible
- There are no field currents dynamic
- There is no cage on the rotor

Electrical sub-system state space model is given below,

$$\frac{d}{dt}\begin{bmatrix} i_d \\ i_q \end{bmatrix} = \begin{pmatrix} -\frac{R}{L_d} & \frac{\omega_r L_q}{L_d} \\ -\frac{R}{L_q} & \frac{\omega_r L_d}{L_q} \end{pmatrix}\begin{bmatrix} i_d \\ i_q \end{bmatrix} + \begin{pmatrix} \frac{1}{L_d} & 0 \\ 0 & \frac{1}{L_q} \end{pmatrix}\begin{bmatrix} v_d \\ v_q \end{bmatrix} + \begin{bmatrix} 0 \\ \omega_r \lambda_{pm} \end{bmatrix} \quad (1)$$

$$T_e = \frac{3}{2}P[\lambda_{pm} i_q + (L_d - L_q) i_d i_q] \quad (2)$$

Mentioned PMSM is non-salient, so q and d inductances are equal, (2) is simplified below.

$$T_e = \frac{3}{2}P\lambda_{pm} i_q \quad (3)$$

Mechanical sub-system transfer function is given below

$$\frac{d}{dt}\begin{bmatrix} \omega \\ \theta \end{bmatrix} = \begin{pmatrix} \frac{-B}{J} & 0 \\ 1 & 0 \end{pmatrix}\begin{bmatrix} \omega \\ \theta \end{bmatrix} + \begin{bmatrix} \frac{1}{J} \\ 0 \end{bmatrix} Te - \begin{bmatrix} \frac{1}{J} \\ 0 \end{bmatrix} T_L \quad (4)$$

B. Linearization and Design of Linear Current Controllers

1) State Feedback Decoupling

The mathematical model of electrical sub-system(1), is non-linear, and therefore can't be represented in linear state space model and in transfer function and linear control systems techniques are not practicable for current control directly [2].

Thus, desired decoupled system is given below

$$\frac{d}{dt}\begin{bmatrix} i_d \\ i_q \end{bmatrix} = \begin{pmatrix} -\alpha_d & 0 \\ 0 & -\alpha_q \end{pmatrix}\begin{bmatrix} i_d \\ i_q \end{bmatrix} + \begin{pmatrix} G_d & 0 \\ 0 & G_q \end{pmatrix}\begin{bmatrix} v_d \\ v_q \end{bmatrix} \quad (5)$$

And applying non-interactive current state feedback linearization to eliminate cross coupling voltages and back EMF feed forward control [6][2]

$$\begin{bmatrix} v_d \\ v_q \end{bmatrix} = \begin{pmatrix} k_{df} & 0 \\ 0 & k_{qf} \end{pmatrix}\begin{bmatrix} u_d \\ u_q \end{bmatrix} - \begin{pmatrix} k_{dd} & k_{dq} \\ k_{qd} & k_{qq} \end{pmatrix}\begin{bmatrix} i_d \\ i_q \end{bmatrix} + \begin{bmatrix} 0 \\ -\omega_r \lambda_{pm} \end{bmatrix} \quad (6)$$

Obtained State feedback gains by replacing (6) into (1) and matching with (5);

$$k_{dd} = \alpha_d L_d - R \quad (7)$$

$$k_{dq} = \omega_r L_q \quad (8)$$

$$k_{qq} = \alpha_q L_q - R \quad (9)$$

$$k_{qd} = \omega_r L_d \quad (10)$$

Obtained feed forward gains;

$$k_{df} = L_d G_d \quad (11)$$

$$k_{qf} = L_q G_q \quad (12)$$

2) Current Control by PIDPseudo Derivative Feedback Controller

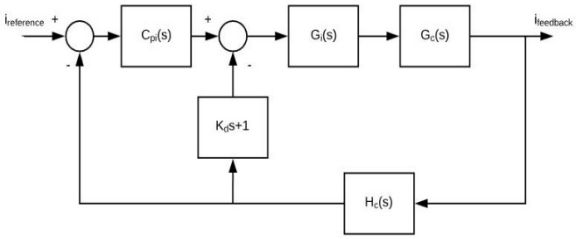


Fig.1. Proposed d and q currents control loop

$C_p(s)$, $G_i(s)$, $G_c(s)$ and $H_c(s)$ represent PI controller, model of inverter, electrical sub-system of PMSM, LPF filter for current feedback. $K_d s+1$ represents pseduo derivative in feedback[10]-[13]. Switching frequency (F_{sw}), sampling frequency (F_{sc}) and sampling period (T_{sc}) of current loop is essential to implement proposed control design. While designing current controllers, it is aimed that transfer function of current control loops are likened to low pass filter with cut off frequency (F_{cc}) and r_i is absolute value of pole of $G_i(s)$

$$C_p(s) = \frac{K_p(s + \frac{K_i}{K_p})}{s} \quad (13)$$

Sampling frequency is equal to (14), [3][7][8] with double updated PWM

$$F_{sc} = 2F_{sw} \quad (14)$$

$$F_{cc} = \frac{F_{sc}}{5} \quad (15)$$

r_i represents absolute value of inverter pole [3][7].

$$r_i = |4F_{sw}| \quad (16)$$

$$G_i(s) = \frac{4F_{sw}}{s + 4F_{sw}} \quad (17)$$

From (5), desired decoupled systems for torque generating,

$$G_c(s) = \frac{1}{L_q s + R} \quad (18)$$

Cut off frequency (F_{cf}) of first order low pass feedback filter,

$$F_{cf} = 5F_{cc} \quad (19)$$

$$H_c(s) = \frac{10\pi F_{cc}}{s + 10\pi F_{cc}} \quad (20)$$

D is coefficient defining place of zeros on root locus applied by PI and C is coefficient defining place of zeros on root locus applied by pseudo derivative feedback.

$$0.9 \geq D \geq 0.1 \quad (21)$$

$$0.9 \geq C \geq 0.7 \quad (22)$$

K_p and K_i, gains and their relations with desired bandwidth (F_{cc}) of current loop, with inductance is defined below. Zero of current PI (Z_{cpi})

$$K_p = 2\pi F_{cc} L_q \quad (23)$$

$$K_i = 2\pi F_{cc} RD \quad (24)$$

$$Z_{cpi} = -D\frac{R}{L_q} \quad (25)$$

PI places zero right side of poles of $G_c(s)$. Therefore, branches of root locus between integrator and PI's zero is real, it is not possible to create imaginary closed loop poles changing gain K_p.

K_d, derivative gain of pseudo feedback and its relations with pole of inverter model and zero replaced by derivative (Z_{cd}) defined below.

$$K_d s + 1 \quad (26)$$

$$K_d = \frac{1}{Cr_i} \quad (27)$$

$$Z_{cd} = -Cr_i \quad (28)$$

Pseudo derivative feedback places zero right side of $G_i(s)$ poles. Therefore, branches of root locus between pole of $G_c(s)$ and zero replaced by derivative feedback is real, it is not possible to create imaginary closed loop poles changing gain K_p

Real axis break-in and breakaway points are calculated as given in [5]

$$\sum \frac{1}{\sigma + z_i} = \sum \frac{1}{\sigma + p_i} \quad (29)$$

Here, z_i and p_i negative of the pole and zero values of open loop system.

In proposed design, imaginary branches of root locus are created between pole of feedback filter and pole of inverter with breakaway points approximately at

$$\sigma \cong \frac{-2F_{sc} - 10\pi F_{cc}}{2} = \frac{-2F_{sc} - 2\pi F_{sc}}{2} = -4.14F_{sc} \quad (30)$$

Current transfer function is 4th order by described design above. More frequencies than desired frequency two polesare recessive complex and two poles are dominant real poles. Because complex poles are recessive their effects on output is suppressed by dominant real pole. One real pole is located between PI's zero and integrator and branch of root locus located between PI's zero and integrator is shorter than other branches of root locus.Therefore, when K_p is muchsmaller than desired K_p satisfying desired bandwidth, one of closed loop poles moving from integrator to PI's zero is located very close to PI's zero. While PI's zero increasing magnitude, closed loop pole decreasing magnitude.Thus, pole and zero eliminate their effect and current transfer function behaves like 3th order system with recessive complex poles, one dominant real pole located between pseudo derivative feedback zero and poles of electrical sub-system. If K_p is increased much more than desired bandwidth, then pseudo feedback derivative's zero and second dominant real pole eliminate their effect as well.Thus, current transfer function behaves like second order system with complex pole and huge overshoot occurs. It is achievable settingcut off frequency of current transfer function between,

$$\frac{F_{sc}}{10} \le F_{cc} \le \frac{F_{sc}}{2} \quad (31)$$

Desirable overshoot or no overshoot occurs, providing that,

$$1kHz \le F_{cc} \le 50kHz \quad (32)$$

C. Design of approximate first order speed control transfer function by PI controller

Overshoot and steady state error are undesirable for speed control. Since, PI controller involves integrator, it guarantees zero steady state error to step signal speed references. Generally, trapezoidal speed reference is used for speed control to soften reference signal. Thus, acceleration feed forward controller is used to minimize following error addition to PI controller as well.

Current loop frequency is at least ten times larger than mechanical sub-system and desired closed speed control, so zeros and poles of current loop are negligible. $T_c(s)$ is current loop designed with natural frequency ω_c, and desired speed loop with natural frequency ω_s

$$\omega_c \square \ \omega_s \quad (33)$$

$$T_c(s) = \frac{\omega_c^2}{s + 2\zeta\omega_c s + \omega_c^2} \quad (34)$$

$$T_c(s)_{s\to 0} = \frac{\omega_c^2}{\omega_c^2} = 1 \quad (35)$$

Since, designed current loop is approximately equal to unity gain, open loop transfer function of speed control is given in(36). $C_{pi}(s)$ is speed PI controller, $G_s(s)$ is first order mechanical sub-system of PMSM, $O_s(s)$ is speed transfer open loop transfer function and $T_s(s)$ is desired transfer function of speed loop.

$$C_{pi}(s)G_s(s) \quad (36)$$

$$G_s(s) = \frac{1/J}{s + B/J} \quad (37)$$

$$C_{pi}(s) = \frac{K_p(s + K_i/K_p)}{s} \quad (38)$$

$$O_s(s) = C_{pi}(s)G_s(s) = \frac{K_p}{J}\frac{s + \frac{K_i}{K_p}}{s(s + \frac{B}{J})} \quad (39)$$

$$T_s(s) = \frac{O_s(s)}{1 + O_s(s)} = \frac{\frac{K_p}{J}(s + \frac{K_i}{K_p})}{s^2 + 2\zeta\omega_s s + \omega_s^2} \quad (40)$$

According to (40), PI controller adds zero to closed loop speed transfer function. If zero is more dominant than poles of closed loop system, resonance peak occurred. Thus, even if there are no complex conjugate poles, overshoot is appeared at closed speed loop response.

To eliminate the effect of zero on closed speed loop response and to guarantee no overshoot, zero is placed between closed loop poles.

E is coefficient providing (41) to place zero closer to imaginary axis than pole of first order system mentioned in(37)

$$0.9 \geq E > 0.1 \qquad (41)$$

Values of K_p and K_i is defined in (42),B, J and ω_s represent viscous friction coefficient, inertia of load and desired bandwidth of closed speed loop.

$$K_p = J\omega_s \qquad (42)$$

$$K_i = B\omega_s E \qquad (43)$$

Replacing (42) and (43)to (39), open loop transfer function is obtained.

$$O_s(s) = \frac{J\omega_s}{J}\frac{s + \frac{B\omega_s E}{J\omega_s}}{s(s + \frac{B}{J})} \qquad (44)$$

Z_{spi} defines place of zero on root locus of speed loop in (45).

$$Z_{spi} = -E\frac{B}{J} \qquad (45)$$

Since, open loop transfer function has one finite zero and two finite poles, there is on asymptote of $O_s(s)$ replacedat,

$$\frac{B}{J}(E-1) \qquad (46)$$

Providing (41), asymptote intersect real axis with degree π radian, thus only asymptote extends over real axis and infinite zero is located on real axis.

From (29) break-in and breakaway points is obtained[5]

$$\frac{1}{\sigma} + \frac{1}{\sigma + \frac{B}{J}} = \frac{1}{\sigma + E\frac{B}{J}} \qquad (47)$$

$$\sigma^2 + 2\sigma E\frac{B}{J} + E\frac{B^2}{J^2} = 0 \qquad (48)$$

Solving (48)

$$\frac{-2E\frac{B}{J} \pm \sqrt{4\frac{B^2(E^2-E)}{J^2}}}{2} \qquad (49)$$

Providing (41) , (49) has imaginary roots. Since, If and only if real break-in and breakaway points are located on real axis [5], there are no real break-in and breakaway points in that design.

Since, in that design no real break-in and breakaway points are occur and all finite and infinite zeros are located on real axis, and all open loop poles are real, all closed loops are located on real axis by changing value ofK_p

F_{cs} is corner frequency of desired speed loop, F_{cc} is corner frequency of designed current loop previous section.

$$F_{cs} = F_{cc}/10 \qquad (50)$$

$$\omega_s = 2\pi F_{cs} \qquad (51)$$

Poles of (40) with conditions described in (41), (42), (43), (50), (51) are located between integrator and zeros of PI (45), and left side of poles of (37) for non-zero gain. Increasing gain, poles moves towards to location of zero, dominant real pole moving to Z_{spi} and recessive real pole moving to infinity zero. For desired bandwidth in (51) dominant real pole is located very closed to right side of $Z_{spi.}$ Thus, closed loop zero and closed loop pole eliminate their effect on closed loop response, second order transfer function behaves like first order system with recessive pole located at $-\omega_s$ which equals to desired bandwidth for speed loop.

D. Design of proportional position controller guaranteeing no overshoot and no steady state error

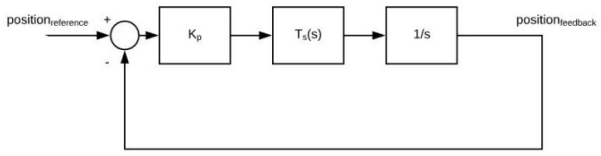


Fig.2. Proposed proportional position controller with unity feedback

In this section, position control loop design without overshoot and steady state error is presented.K_p, $T_s(s)$represent proportional gain of position controller, designed closed loop speed control. Approximated first order closed speed loop is given below

$$T_s(s) = \frac{\omega_s}{s + \omega_s} \qquad (52)$$

Open loop transfer function of position loop is,

$$G_p(s) = K_p T_s(s) F_p(s) = K_p \frac{\omega_s}{s + \omega_s}\frac{1}{s} \qquad (53)$$

Open loop transfer function has two poles, integrator and three infinity zeros. From (29),

$$\frac{1}{\sigma + \omega_s} + \frac{1}{\sigma} = 0 \qquad (54)$$

$$\sigma = -0.5\omega_s \qquad (55)$$

By increasing proportional gain K_p closed loop poles move from open loop poles, where K_p is equal to zero, to zeros of systems where K_p is equal to infinity. [5] While increasing K_p for damping ratio over one, all closed loops are real, and for damping ratio under one all closed loops are complex conjugates pole. Characteristic equation of closed position loop is given (56) and desired characteristic equation of closed position loop is given

$$C_r(s) = s^2 + \omega_s s + K_p\omega_s \qquad (56)$$

$$C_d(s) = s^2 + 2\zeta\omega_p s + \omega_p^2 \qquad (57)$$

ζ represents damping ratio and ω_p representsnatural frequency of second order position transfer function. Minimum value of damping ratio is equal to one for system response without overshoot [5]. Bandwidth

and natural frequency relation of second order system is given below[5]

$$BW = \omega_p \left[(1-2\zeta^2) + \sqrt{4\zeta^4 - 4\zeta^2 + 2} \right]^{\frac{1}{2}} \quad (58)$$

$$\zeta = 1 \quad (59)$$

Providing (59), bandwidth and natural frequency relation is given in[5]

$$BW = 0.64\omega_p \quad (60)$$

(60)showsmaximum possible bandwidth with no overshoot. Providing (59) and matching between (56) and (57)

$$s^2 + \omega_s s + K_p \omega_s = s^2 + 2\omega_p s + \omega_p^2 \quad (61)$$

$$\omega_p = 0.5\omega_s \quad (62)$$

$$K_p \omega_s = \omega_p^2 \quad (63)$$

Replacing (62)in(63)

$$K_p = \frac{\omega_s}{4} = \frac{\omega_p}{2} \quad (64)$$

Maximum K_p for no overshoot is equal to quarter of natural frequency of speed loop and half of desired natural frequency of position loop.

From (60) and (62) for maximum K_p desired closed loop maximum bandwidth is given below [5], [9]

$$BW = 0.32\omega_s \quad (65)$$

III. MEASUREMENT OF SPEED AT FOR LOW SPEED CONTROL

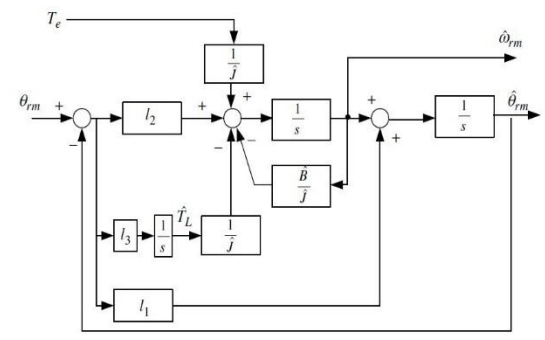


Fig.3.Full order speed observer block diagram [3]

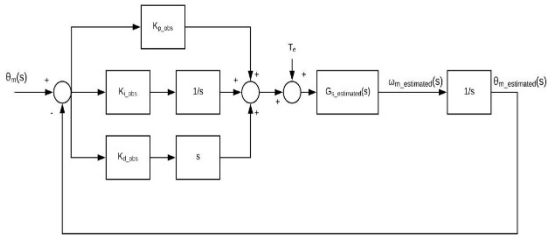


Fig.4. Full order speed observer in PID form

Resolution of encoder is significant at low speed control.Conventional speed measurement techniques, such as T method, measures time interval between adjacent pulses and calculates speed by arithmetic division [3]. For reason that time interval between pulses increased largely at low speed, so quality of measurement is decreased.

Therefore, full order Luenberger observer to measure speed is proposed. Moreover, full order Luenberger speed observer is liken to PID controller and is similarly tuned PID controller [3]. Mentioned speed observer consists of estimated mechanical sub-system $\hat{G}_s(s)$, output of estimatedmechanical sub-system is equal to estimated mechanical speed $\hat{\omega}_m(s)$ (radian/s) and by integrating estimated speed, estimated position $\hat{\theta}_m(s)$ (radian) is obtained. Real position measured by encoder $\theta(s)$ (radian) and estimated position $\hat{\theta}_m(s)$ represent reference and feedback signal of PID liked speed observer. T_L represents load torque providing (66), and mechanical sub-system's state space model is given in (67), [3]

$$\frac{dT_L}{dt} \approx 0 \quad (66)$$

$$\frac{d}{dt}\begin{bmatrix} \hat{T}_L \\ \hat{\omega}_m \\ \hat{\theta}_m \end{bmatrix} = \begin{pmatrix} 0 & 0 & 0 \\ 0 & -\frac{\hat{B}}{\hat{J}} & 0 \\ 0 & 1 & 0 \end{pmatrix} \begin{bmatrix} \hat{T}_L \\ \hat{\omega}_m \\ \hat{\theta}_m \end{bmatrix} + \begin{bmatrix} 0 \\ 1 \\ 0 \end{bmatrix} [T_e] + \begin{bmatrix} L_3 \\ L_2 \\ L_1 \end{bmatrix} \left(\theta_m - \hat{\theta}_m \right) \quad (67)$$

State space model of general Luenberger observer is given in (68)and (69).

$$\frac{d\hat{x}}{dt} = (A - LC)\hat{x} + Bu + Ly \quad (68)$$

$$\hat{y} = C\hat{x} \quad (69)$$

Using equations and, full order speed observer state space model is obtained [3][5]. States of speed observer are position, speed and load torque. Thus, speed observer also observes load torque and position. However, bandwidth of speed observer must be much more than (83) to observe load torque fast.

$$\frac{d}{dt}\begin{bmatrix} \hat{T}_L \\ \hat{\omega}_m \\ \hat{\theta}_m \end{bmatrix} = \begin{pmatrix} 0 & 0 & -L_3 \\ 0 & -\frac{\hat{B}}{\hat{J}} & -L_2 \\ 0 & 1 & -L_1 \end{pmatrix} \begin{bmatrix} \hat{T}_L \\ \hat{\omega}_m \\ \hat{\theta}_m \end{bmatrix} + \begin{bmatrix} 0 \\ 1 \\ 0 \end{bmatrix} [T_e] + \begin{bmatrix} L_3 \\ L_2 \\ L_1 \end{bmatrix} (\theta_m) \quad (70)$$

Gains of given speed observer in PID form in figure 3. isgiven below [3]

$$K_{d_obs} = l_1 \hat{J} \quad (71)$$

$$K_{i_obs} = l_3 \quad (72)$$

$$K_{p_obs} = l_2 \hat{J} \quad (73)$$

Open loop transfer function of speed observer with two integrator is given in (74) and its transfer function is third order system with two zeros represented in (75)

$$\frac{K_{d_obs} s^2 + K_{i_obs} s + K_{p_obs}}{s^2 (\hat{J}s + \hat{B})} \quad (74)$$

$$\frac{\hat{\theta}_m(s)}{\theta_m(s)} = \frac{K_{d_obs}s^2 + K_{i_obs}s + K_{p_obs}}{\hat{J}s^3 + (\hat{B} + K_{d_obs})s^2 + K_{i_obs}s + K_{p_obs}} \quad (75)$$

That design represented in (74) consists of three finite poles, two finite zeros and one infinite zeros.
Placing double zeros on point mentioned in (76)

$$z_{1,2} = -F\frac{\hat{B}}{\hat{J}} \quad (76)$$

By placing (76) into (74)

$$O_{obs}(s) = \frac{K_d(s + F\frac{\hat{B}}{\hat{J}})^2}{s^2(s + \frac{\hat{B}}{\hat{J}})} \quad (77)$$

Real axis break-in and break away points are given[5],

$$\frac{2}{\sigma} + \frac{1}{\sigma + a} = \frac{2}{\sigma + Fa} \quad (78)$$

$$\sigma^2 + 3F\frac{B}{J}\sigma + 2F\frac{B^2}{J^2} = 0 \quad (79)$$

Solving (79) for values of F is represented in (80)

$$F \geq \frac{8}{9} \quad (80)$$

Break-in point is occurred approximately at $-1.34\,\hat{B}/\hat{J}$ on real axisfor values of $F = 8/9$ and complex break away points occurred to double integrator, changing K_d from zero to infinity closed loops poles moves from double integrator to finite zeros and third closed loops poles moves from $-\hat{B}/\hat{J}$ to infinite zero on real axis.
Thus, according to (79) values of F providing (81)

$$\frac{8}{9} > F > 0 \quad (81)$$

real axis break-in and break away points are not occurred, only complex break-in point at location of double zeros and only complex breakaway point at location of double integrator are occurred [5]. Providing that (82)

$$K_d = 0 \quad (82)$$

Closed loop poles are equal to open loop poles, increasing K_d two closed loop poles moves from double integrator to double zeros located at $-F\hat{B}/\hat{J}$ and other closed loop poles moves from $-\hat{B}/\hat{J}$ to real infinite zero
Moreover, bandwidth of speed observer is preferred to be equal at least three times of speed loop. Desired bandwidth of observer is given [3][7]

$$\omega_{obs} = 3\omega_s \quad (83)$$

$$\omega_s = \frac{\omega_c}{10} \quad (84)$$

Replacing (83)in(84),(85) is obtained

$$\omega_{obs} = \frac{3\omega_c}{10} \quad (85)$$

Providing(85)and (32)

$$\omega_{obs} > 1880 rad/s \quad (86)$$

Third order transfer function is approximated to first order transfer function, Since, two imaginary poles are very close to finite double zeros, recessive poles characterize behavior at system at location $-\omega_{obs}$. [5][9]

$$K_d \cong \omega_{obs}\hat{J} \quad (87)$$

IV. SIMULATIONS AND RESULTS

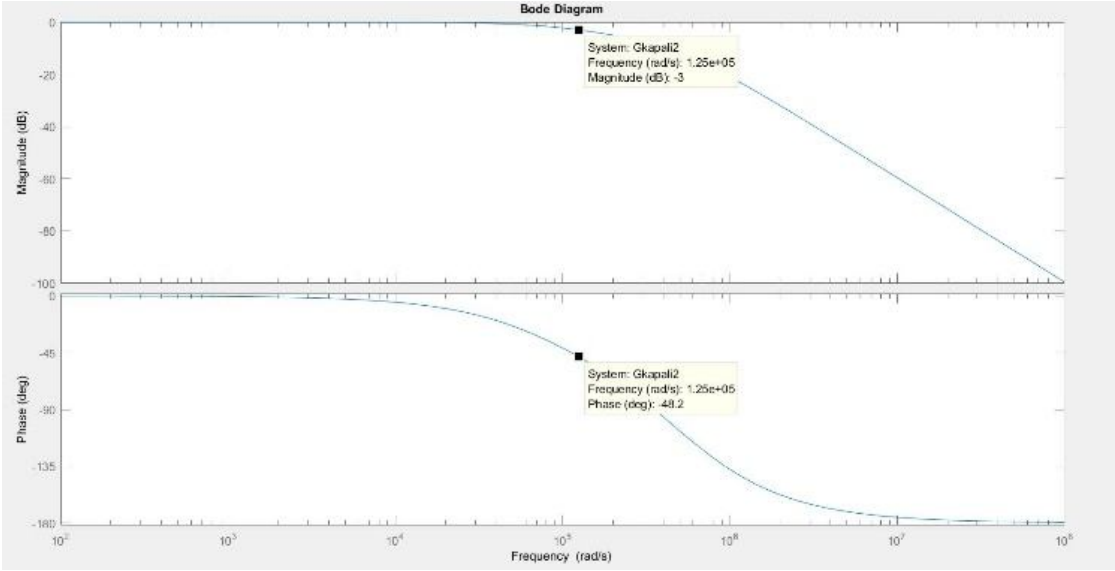


Fig.5. Current Loop with 125000 radian/s bandwidth

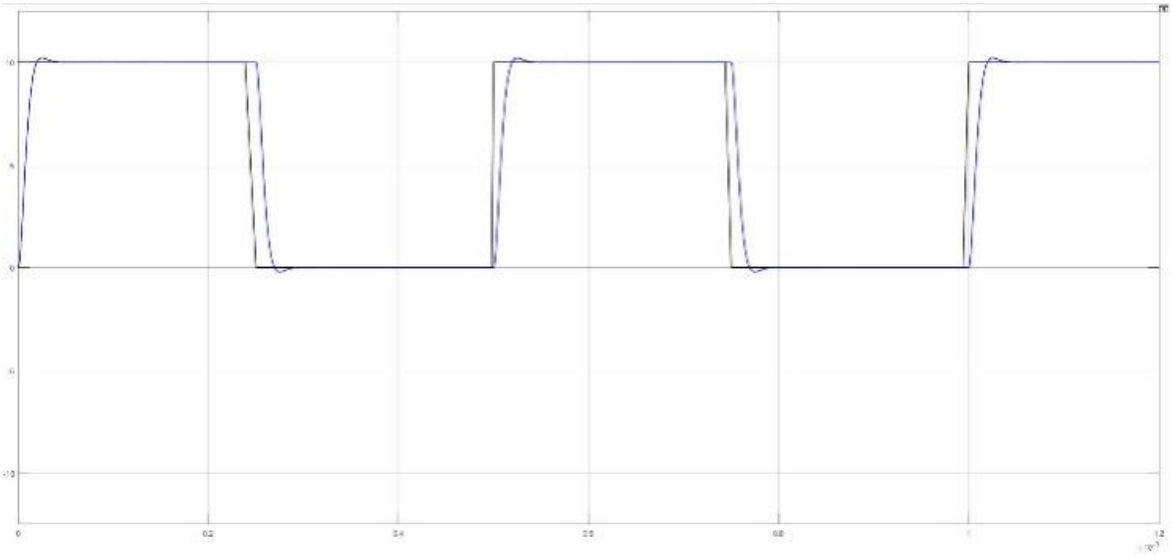


Fig.6. Response of Current Loop to 2kHz torque generating pulse reference

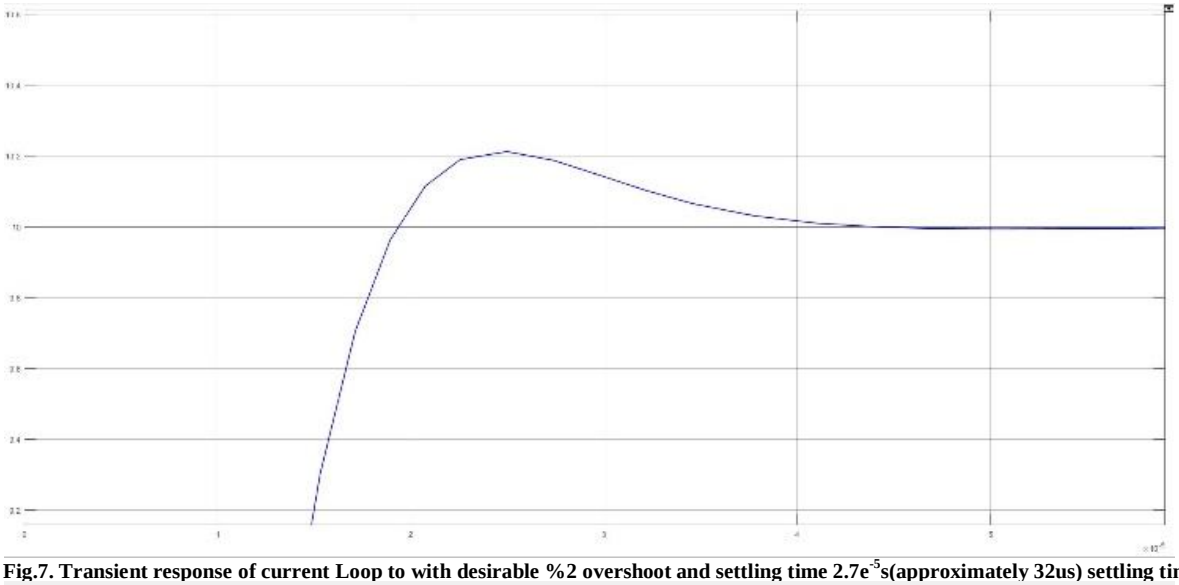


Fig.7. Transient response of current Loop to with desirable %2 overshoot and settling time $2.7e^{-5}$s(approximately 32us) settling time

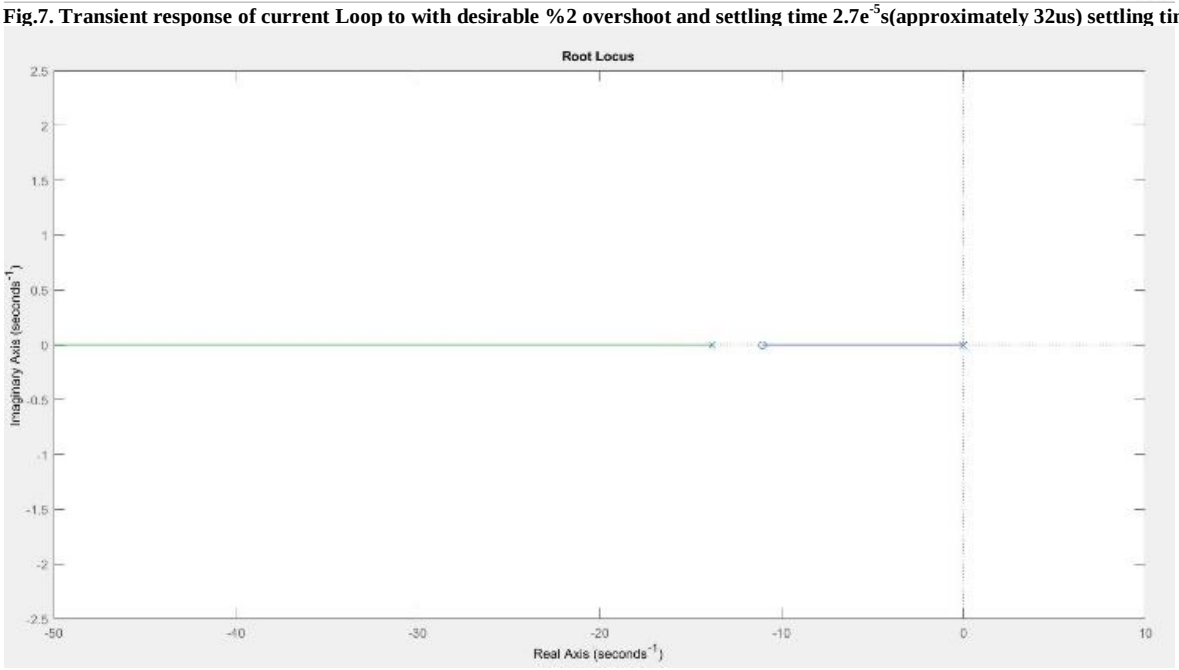


Fig.8. Root Locus of Speed Loop

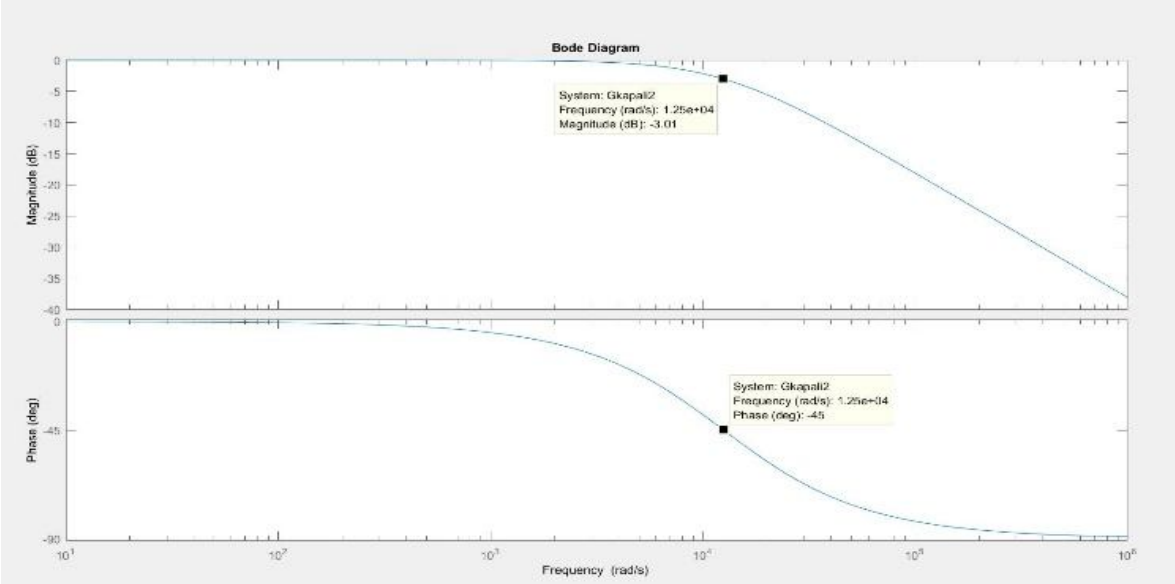


Fig.9. Bode of Speed Loop with 12500 radian/s bandwidth

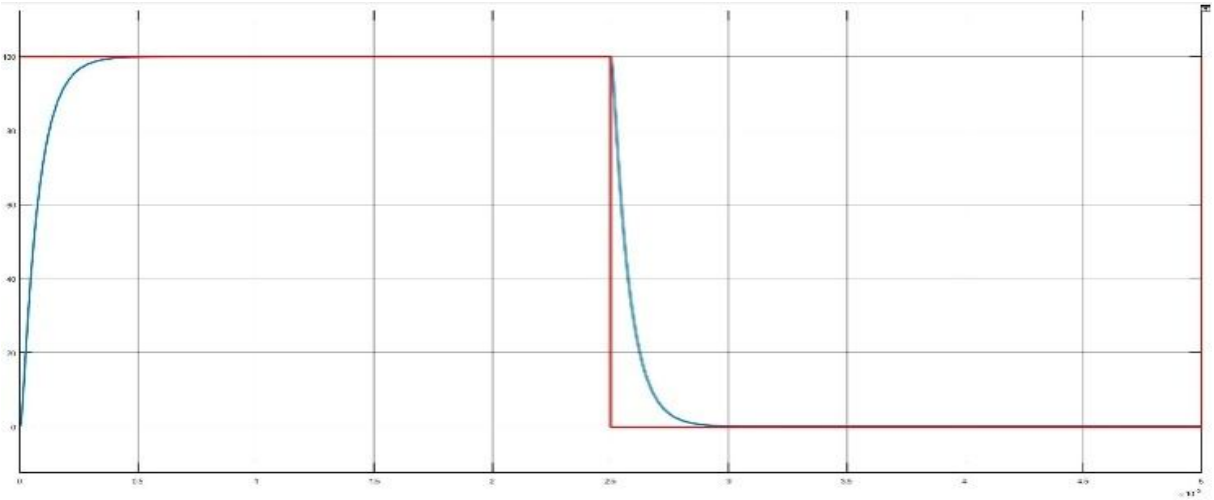


Fig.10. 100radian/second speed reference with 200Hz frequency and speed feedback

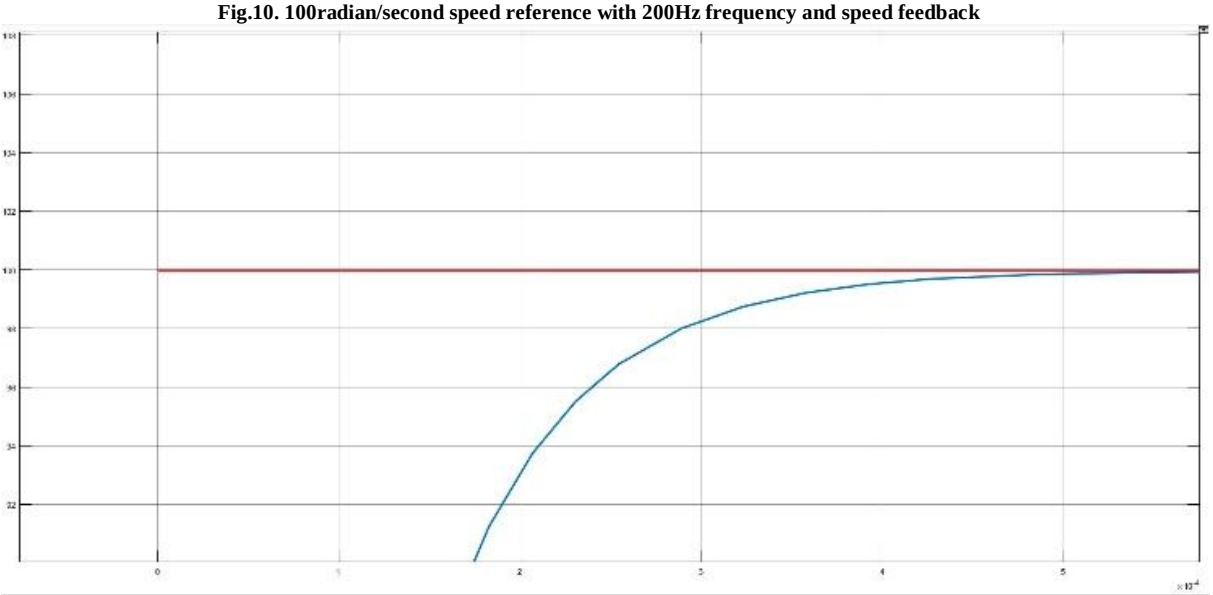


Fig.11. Settling time of Speed Loop approximately 320us (2.8e^{-4}s)

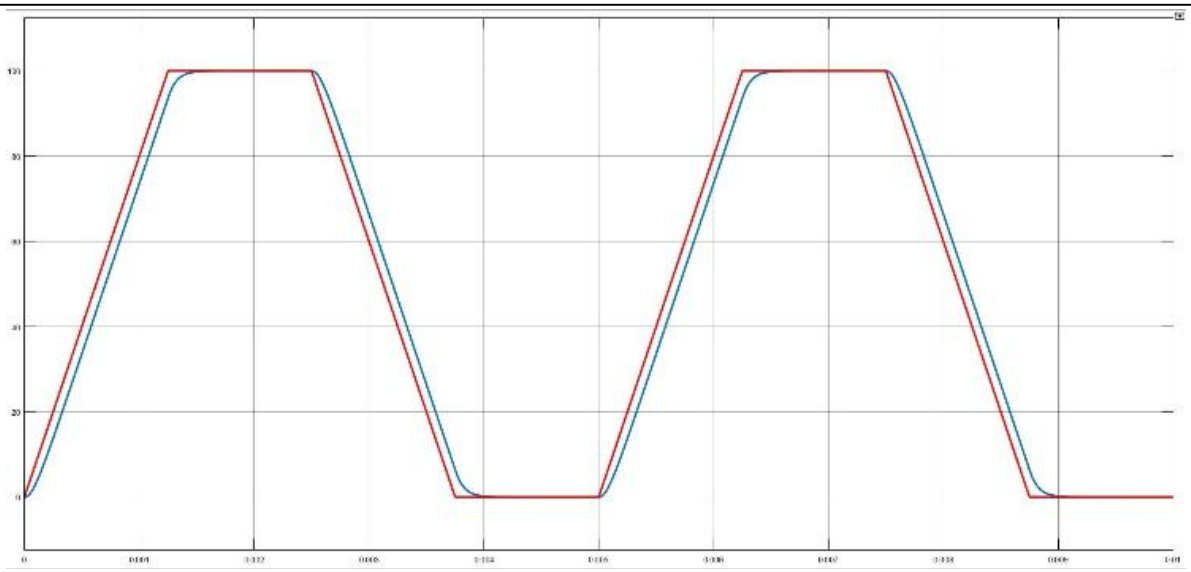


Fig.12. 100 radian/ seconds trapezoidal speed reference with 200 Hz frequency and speed feedback.

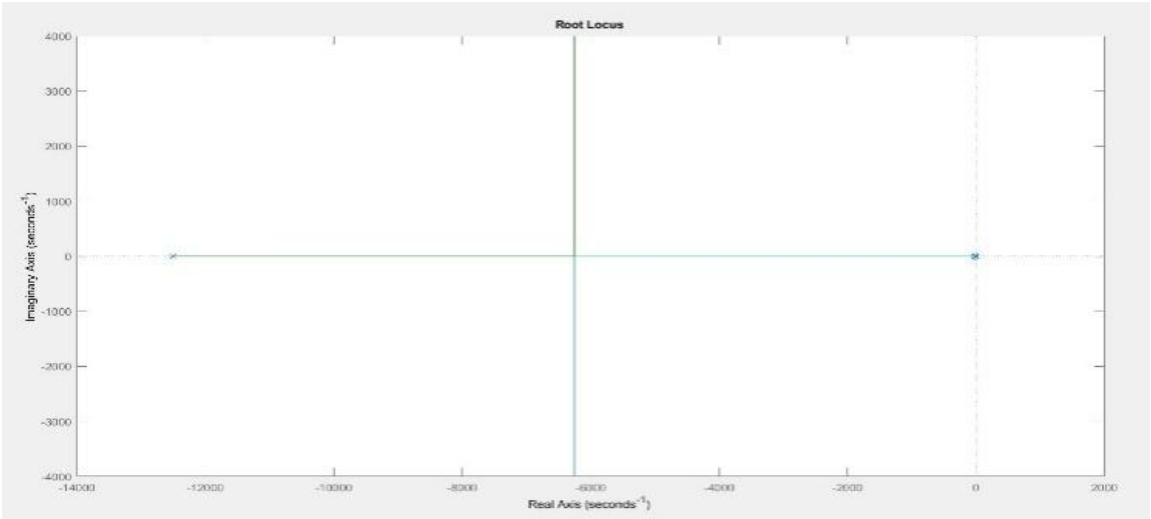


Fig.13. Root locus of position loop.

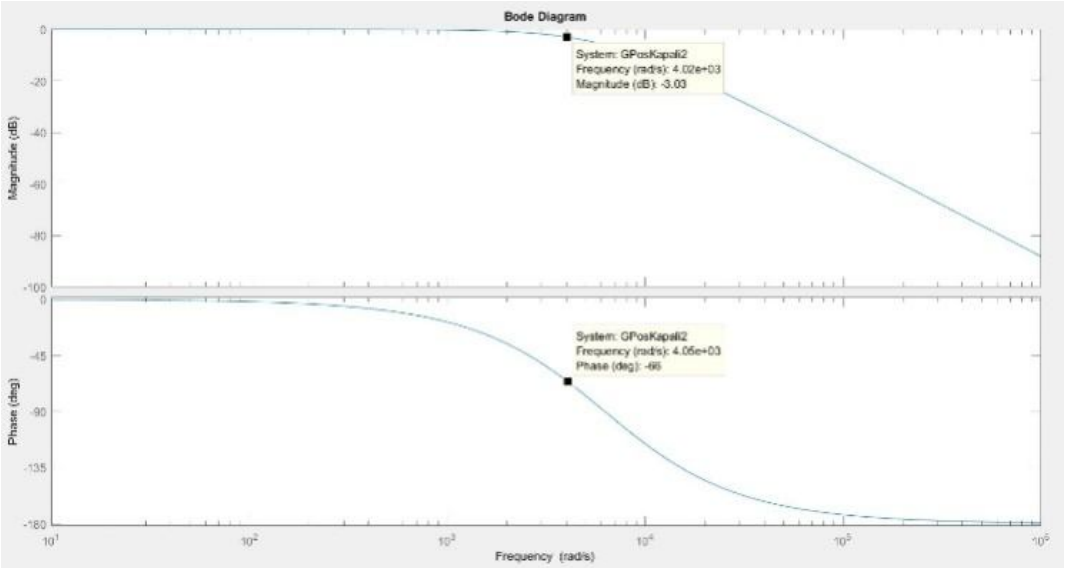


Fig.14. Bode of position loop with 4000radian/s cut off frequency.

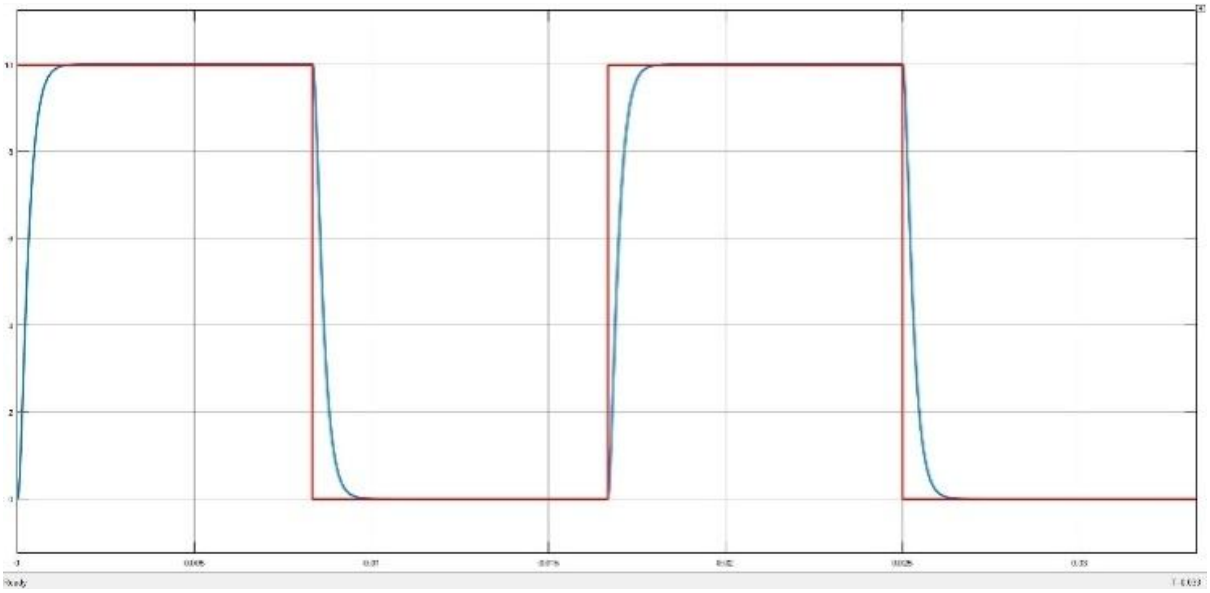


Fig.15. 10radian position reference with 60Hz frequency and position feedback.

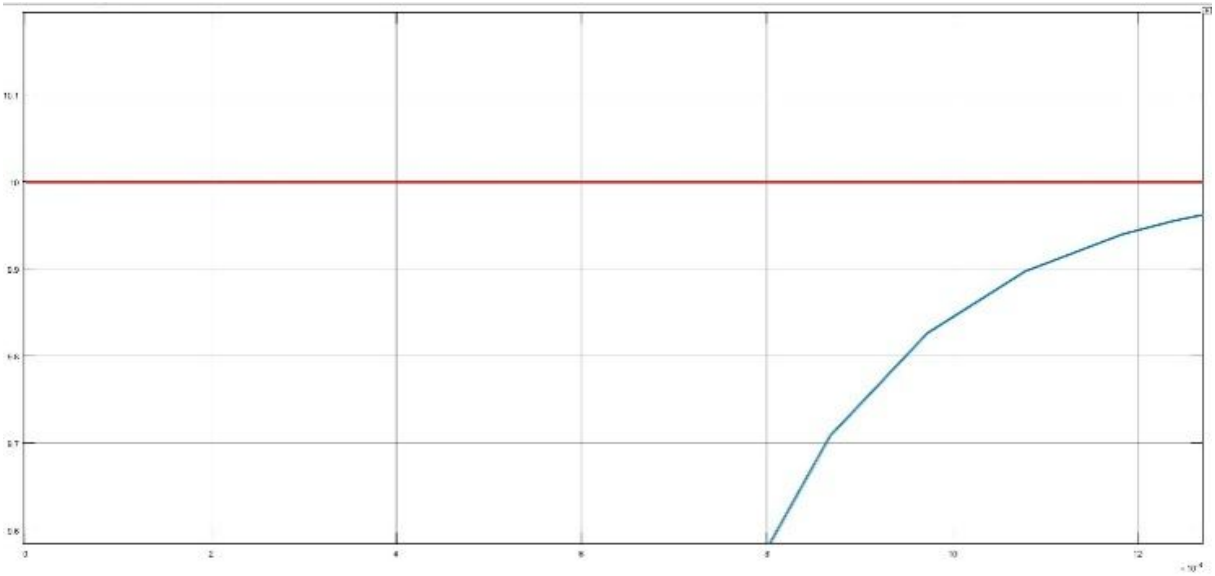


Fig.16. Position loop settling time 9.2e-4 (approximately 1ms).

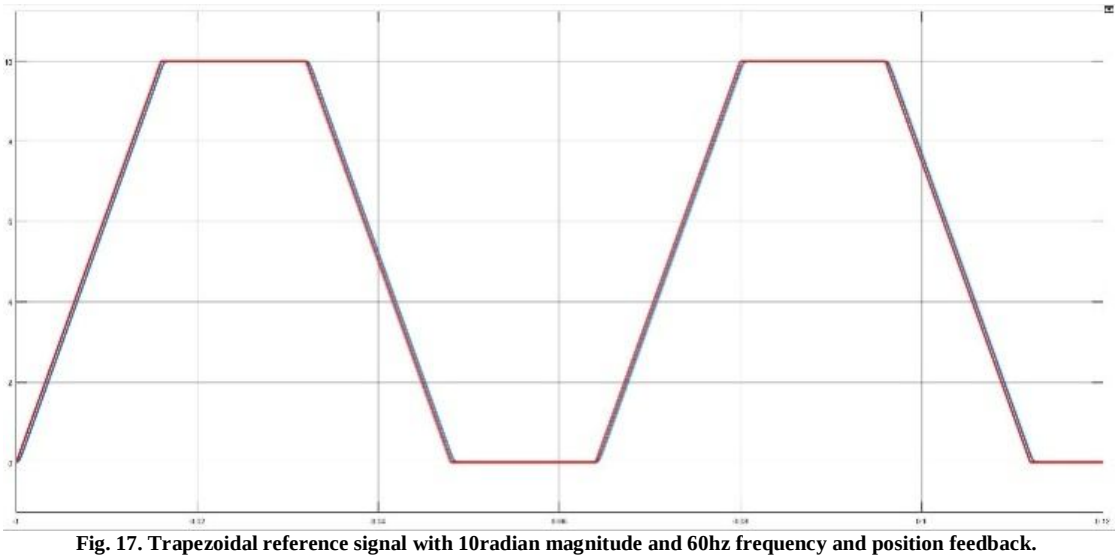


Fig. 17. Trapezoidal reference signal with 10radian magnitude and 60hz frequency and position feedback.

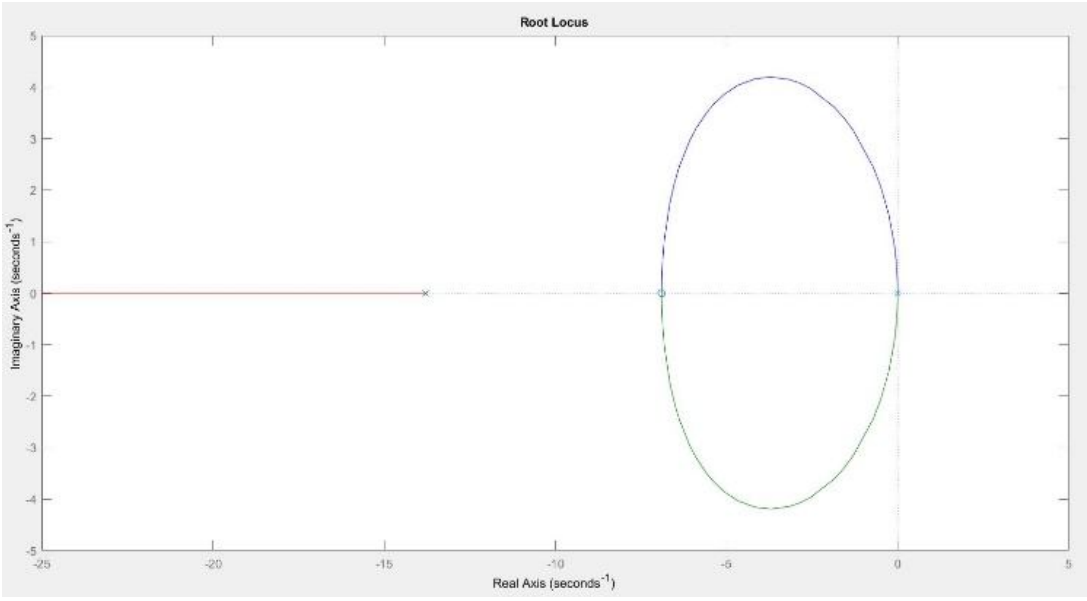


Fig. 18. Root locus of speed observer.

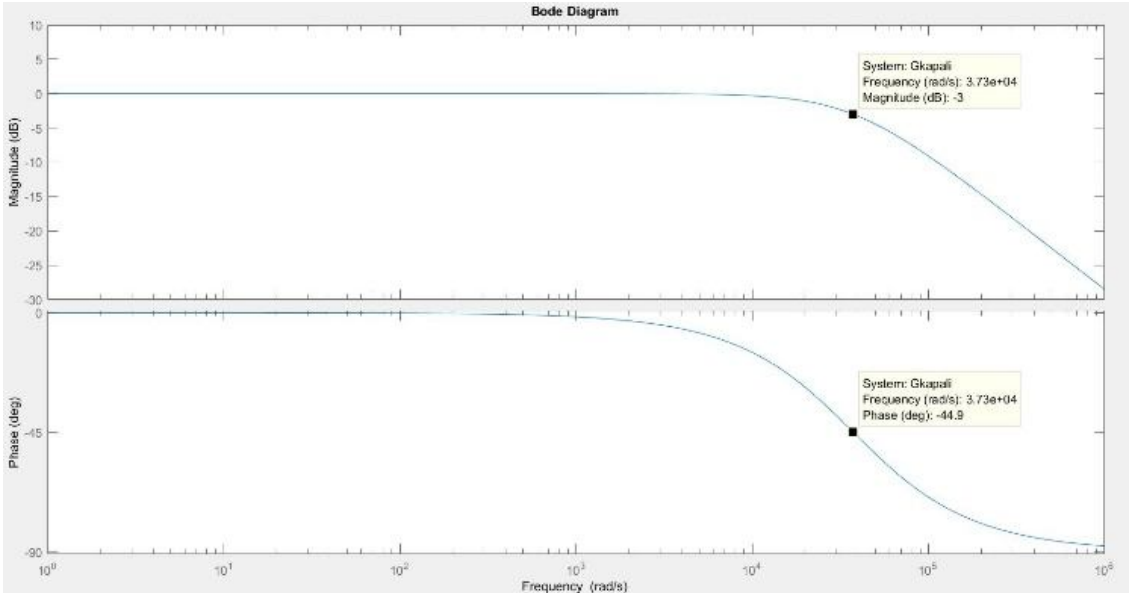


Fig.19. Bode of speed observer with 37300 radian/s bandwidth

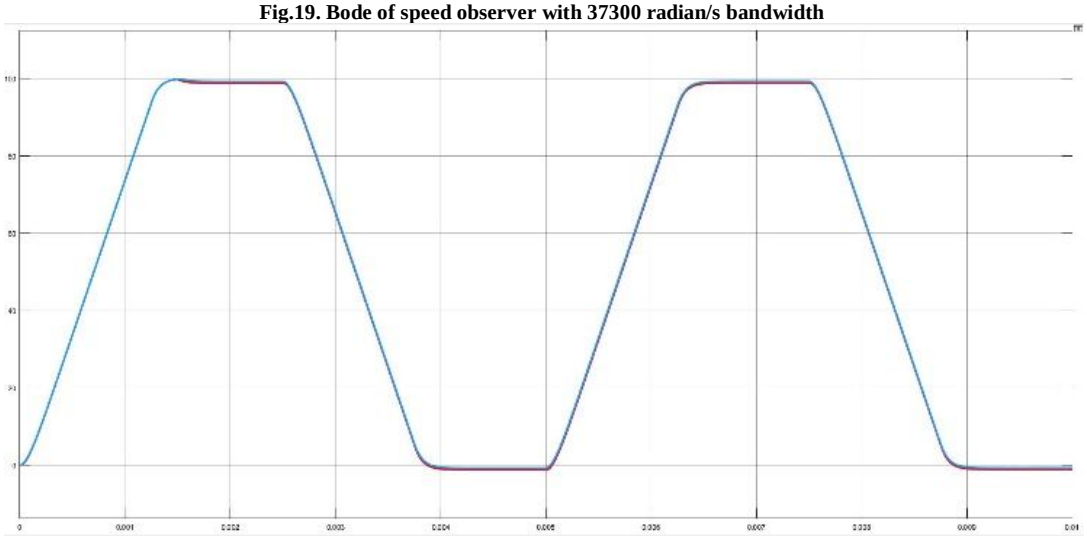


Fig.20. 200 Hz Real Speed Feedback and Estimated Speed Feedback with applied load torque at 0.015 seconds

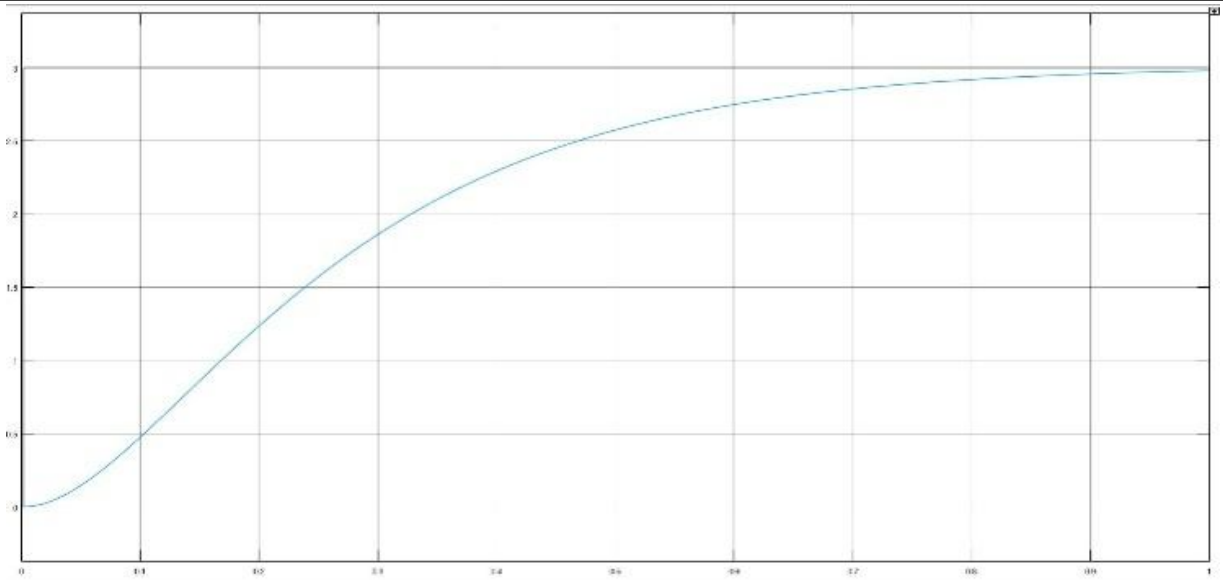


Fig. 21. Speed Observer with 37300 radian/s bandwidth, load torque estimation performance, estimation of load torque 0.8 seconds approximately

In simulation, position loop with 1ms settling time, speed loop with 320us settling time, current loop 32 us settling time and speed observer with 100us settling time is design. For that design bandwidth of position loop is approximately 4000radian/s, speed loop is approximately 12500 radian/s,

Speed observer is approximately 37500 radian/s and current loop is approximately 125000 radian/s. 50khz switching frequency and 100khz sampling frequency for current loop are required.

REFERENCES

[1] K. Sakata, H. Fujimoto, L.Peretti, M. Zigliotto, "Enhanced Speed and Current Control of PMSM Drives by Perfect Tracking Algorithm," The 2010 International Power Electronics Conference, pp. 588-592

[2] P. Ramana, K.A. Marry, M.S. Kalavathi, "State Feedback Linearization of a Non-linear Permanent Magnet Synchronous Motor Drive,"Indonesian Journal of Electrical Engineering and Computer Science, vol.1, No.3, pp. 534-542, March 2016

[3] S. SUL, Control of Electric Machine Drive Systems, IEEE Press,2011.

[4] A. Kamalselvan, S. L. Prakash, "Modelling Simulation and Analysis of Closed Loop Speed Control of PMSM Drive System,"International Conference on Circuit, Power and Computing Technologies", 2014

[5] N. S. Nise, "Control Systems Engineering", 6th Edition, John Wiley & Sons Inc., 2011

[6] H. J. Marquez, "Nonlinear Control Systems Analysis and Design", John Wiley & Sons Inc., 2003

[7] G. Ellis, "Control System Design Guide", 3th edition, Elsevier Academic Press, 2004

[8] R. Krishnan, "Electric Motor Drives Modelling, Analysis and Control", Prentice Hall, 2001

[9] B. C. Kuo, F. Golnaraghi, "Automatic Control Systems" 9th Edition, John Wiley & Sons Inc., 2010

[10] T. Kubota,K. Y. ToumiLimitation of linear controllers for the precision magnetic bearing with uncertainties. Proc. the American Contr. Conf. Philadelphia, Pennsylvania, June 1998, pp. 2204-2228

[11] Aydin Y., Gurleyen F.,Adaptive Variable Structure Control of Active Magnetic Bearings for Rigid Rotors with Uncertain External Payloads, Proceedings of the 2017 IEEE International Conference on Mechatronics (ICM), Australia, 2017.

[12] P.A.Ioannou, J. Sun, Robust Adaptive Control, Prentice Hall PTR, Upper Saddle River, NJ, 1996.

[13] Zhou K., Doyle J.C., and Glover K., Robust and Optimal Control, Prentice Hall Inc, Upper Saddle River, NJ, 1996.

[14] J. Wang, J. D. Yan, L. Jiang, "Pseudo-Derivative-Feedback Current Control for Three-Phase Grid-Connected Inverters with LCL Filters

[15] A. Karthikeyan, K. K. Prabhakaran, B. P. Venkatesa, C. Nagamani, "Pseudo Derivative Feedback Current Controlled Sensorless PMSM Drive with Flux-Torque based MRAS estimator for low speed operation", SLED, 2017

[16] W. L. Brogan, "Modern Control Theory", 3th Edition, Prentice Hall, 1991

[17] S. Song, S. Sul, "An Instantaneous Speed Observer for Low Speed Control of AC Machine", IEEE, 1998

★★★